Micro-structural and compositional study: ε-Fe_2O_3 crystals in the Hare's Fur Jian Ware

Shiqian Tao
Shanghai Institute of Optics and Fine Mechanics Chinese Academy of Sciences
Song Liu
Shanghai Institute of Optics and Fine Mechanics Chinese Academy of Sciences
Yimeng Yuan
Shanghai Institute of Optics and Fine Mechanics Chinese Academy of Sciences
Junqing Dong
Shanghai Institute of Optics and Fine Mechanics Chinese Academy of Sciences
Qing-Hui Li (qinghuil@sina.com)
Shanghai Institute of Optics and Fine Mechanics Chinese Academy of Sciences
https://orcid.org/0000-0002-1007-3487

Research Article

Keywords: Jian ware, Hare's fur, epsilon hematite, microstructure

Posted Date: December 6th, 2021

DOI: https://doi.org/10.21203/rs.3.rs-1130777/v1

Abstract

The Jian kilns in the present-day Jianyang county of Fujian province are well-known as their thick and lustrous black-glazed porcelain production. The hare's fur (HF) glazed Jian wares characterized by radial fur-like strips, as one of the most typical representatives of black-glazed tea bowls, are originated from phase separation of glaze melt and crystallization of iron oxides. In this work, various techniques were performed on the yellowish-brown HF samples, including portable energy-dispersive X-ray fluorescence (PXRF), synchrotron X-ray absorption near-edge spectroscopy (XANES), optical microscopy (OM), scanning electron microscopy (SEM), X-ray diffraction (XRD) and Raman spectroscopy (RS). The objective of this study was to well understand the microstructure characteristics and chemical compositions of glaze patterns. Results showed that the main constituents of the ceramic glaze were alumina (10.61-16.43 wt.%), silica (62.20-77.07 wt.%), calcium (3.85-6.97 wt.%) and iron oxide (4.10-8.35 wt.%). The studies evidenced that the presence of metastable epsilon-hematite crystals (ε-Fe_2O_3) formed on the brownish yellow glazed surface. Microstructural analysis revealed that there were three types of crystal structures in the glaze surface, one consisted of well-grown leaf-like or dendritic-like structure with highly ordered branches at micrometers scales, one was comprised of flower-like clusters accompanied by branches radiating from the center, petals growing along the branches and needles on both sides of the petals, and the last embraced a honeycomb structure tightly packed with plentiful spherical or irregular-shaped particles. In addition, ε-Fe_2O_3 crystals in the cross-section of glaze showed a gradient distribution.

1. Introduction

The Jian kiln is located in present-day Jianyang county of Fujian province, one of the representative folk kiln of producing black-glazed tea bowls. This kiln began firing porcelain in the Tang dynasty (618-907 A.D.), manufactured particularly during the Southern Song dynasty (1127-1279 A.D.) and closed down in the Yuan dynasty (1271-1368 A.D.)[1]. In the Song Dynasty, due to the abundant raw materials, low prices and the prevailing trend of tea tasting and competition, the production of black-glazed tea bowls increased greatly. The prevalence of these Jian wares also reflected the pursuit of simplicity and elegance. Apart from their thick and lustrous black glaze, Jian wares are greatly appreciated due to the striking streaked or mottled patterns, generally recognized as "Hare's fur (HF)", "oil spot (OS)", and "partridge spot"[2,3]. Different glaze decoration effects can be achieved by changing the firing schedules to modify the crystallization behavior and microstructure of the glazes[4–6]. Among these, "Hare's fur" is the most common and famous variety, recognized by a sparkling black glaze showing fine radial rust-colored fur-like strips. HF patterns are encountered in the black glaze due to the phase separation and crystallization during the firing process in the dragon kiln[5].

The Hare's fur glaze is one kind of ferric phase separation glaze. This unique colored patterns are inevitably derived from local iron-enrichment raw materials and firing process. During the high temperature firing process, the glaze begins to melt and the iron oxides in the glaze decompose to give

off oxygen once the temperature reaches 1240℃, oxygen bubbles in the glaze layer continuously generate and grow up during the heating stage, and the concentration of iron-rich oxides around the bubbles improves gradually. Eventually, the large bubbles move out within the molten glaze and carry iron towards the surface, forming a local iron-rich area on the glaze[7–9]. Because of the low viscosity at certain spots, iron oxides supersaturate and crystallize on the glaze surface during the cooling stage, forming the iron-rich streaks. Meanwhile, the surface iron-rich areas begin to flow down along the sides of the bowl. The control of the atmosphere during the firing process (oxidizing and/or reducing) will have a significant impact on the color of streaks. In 2014, the aggregate crystals in the Hare's fur glaze were firstly confirmed as metastable epsilon-hematite (ε-Fe_2O_3) rather than the most thermally stabled iron oxide phase (α-Fe_2O_3)[10]. ε-Fe_2O_3 only existed in nanoparticles, nanorods, nanowires or thin films form has recently received growing attention due to the significant and promising magnetic properties such as giant coercive field of around 2T at room temperature, magneto-resistance or millimeter-wave ferromagnetic resonance (FMR) absorption[11–14].

It is worth mentioning that subsequent studies on ε-Fe_2O_3 in ancient Chinese porcelains have been carried out to understand the formation process and color variation of glaze patterns[15]. The crystalline markings of precipitated iron oxide on Hare's fur glazed bowl sherds excavated from the Jian kiln are organized orderly in well-grown leaf-like or dendritic-like manners in a micrometer size, some typically present in the form of millimeter-sized flower-like clusters[16]. Interestingly, surface crystals of HF samples exclusively consist of ε-Fe_2O_3 microcrystals, which are significantly larger than the currently synthetic ε-Fe_2O_3 nanoparticles[10]. ε-Fe_2O_3 has become a research hotspot as the chromogenic crystals. Researchers also reported the existence of ε-Fe_2O_3 polymorph in the oil spot Jian wares[17], sauce glaze porcelain from the Qilizhen kiln[18], rusty oil spotted glaze at the Linfen kiln[19] and/or Xiao kiln[20], Hare's fur glaze of Jizhou kiln[21], brown glaze porcelain of Yaozhou kiln[22], sauce glaze and black glaze porcelains from Qingliangsi site[23], and purple-gold glaze porcelain from the Forbidden City[24]. It is believed that researches on the growth mechanism of ε-Fe_2O_3 in ancient porcelains will not only provide guidance for the artificial synthesis on this promising material, but also have a profoundly influence on the Asian ceramic history.

In this work, a representative fragment of yellowish-brown hare's fur Jian ware was selected to further study the forming cause and growth process of glaze patterns using a variety of characterization methods, since the existing researches were mostly focused on one type of glaze in different kilns or the comparison of porcelains with distinguishing glaze patterns, lacking the comprehensive and deeply analysis on the micro-structural and compositional studies of ε-Fe_2O_3 crystals. This basic research may provide some useful insight for scientific researches of other ancient Chinese porcelain.

2. Materials And Methods

2.1 Sample preparation

Archaeological fragments of the brownish colored Hare's fur glaze bowl (Fig. 1, labeled the HF sample) excavated from Jian kiln relics (Jianyang District, Nanping City, Fujian Province) were brought to the laboratory for the analysis, which were supposed to be belonged to Song Dynasty (960-1279 A.D.). The tested zone of sample was cut by water cutting machine into small pieces to do the following experiments. Some specimens supplied with the observation of the cross-sections needed to be impregnated with epoxy, and then finely polished by routine metallographic methods.

2.2 Characterization techniques

Portable energy-dispersive X-ray fluorescence spectroscopy (PXRF, OURSTEX 100FA, OURSTEX, Japan) was applied to analyze the chemical composition of glaze and body of the HF sample (the concentration of light elements such as Na and Mg can be measured by this PXRF instrument[25,26]). It was equipped with a low-vacuum sample chamber, can effectively reduce the absorption of characteristic spectra of light elements in air.

Synchrotron X-ray absorption near-edge spectroscopy (XANES) was employed to identify the valence state of iron in the Hare's fur glaze. The Fe K-edge XANES spectra were collected at the beam line station BL15U1, Shanghai Synchrotron Radiation Facility (SSRF), Chinese Academy of Sciences, China. In this experiment, XANES spectra were obtained in the fluorescence yield mode together with Lytle detector. 28 points were measured with a scanning step of 50 μm, the acquisition time of each energy point was 2 s. Particularly, the scanning area was approximately in the range of 7050-7349.5 eV and the step size was 0.5 eV.

The surface morphology of the porcelain sample was firstly examined by optical microscope equipped with an ultra-depth-of-field system (OM, VHX-50000, Keyence, Japan). Images can be taken with a magnification ranging from ×20 to × 1000. The microstructure and elemental composition of crystals in glaze were performed by scanning electron microscope (SEM) fixed with energy-dispersive X-ray spectroscopy (EDS) operated in back scattered electron image mode (TM3000, HITACHI, Japan). Secondary electron images with higher magnification were obtained by another SEM equipment (SU8220, HITACHI, Japan).

The information on phase constituents of the glaze was characterized by an X-ray diffractometer (XRD, D/max 2550V, Rigaku, Japan) with filtered Cu Kα (40 kV, 40 mA) radiation at a scan rate of 0.5° min^{-1} in the 2θ range of 20-80°. The Raman spectra were collected using a Laser Confocal Micro-Raman spectrometer (LabRAM XploRA, Horiba, France), and a diode near-infrared (NIR) (532 nm) laser was used for the excitation.

3. Results

3.1 Chemical composition

As shown in Table 1, the main constituent of Hare's fur glaze area was probably 62.20 wt.% SiO_2, 16.43 wt.% Al_2O_3, 8.35 wt.% Fe_2O_3, 3.02 wt.% K_2O and 6.97 wt.% CaO, and the black glaze area mainly consisted of 77.07 wt.% SiO_2, 10.61 wt.% Al_2O_3, 4.10 wt.% Fe_2O_3, 2.06 wt.% K_2O and 3.85 wt.% CaO. The body contained approximately 66.32 wt.% SiO_2, 18.50 wt.% Al_2O_3, 10.04 wt.% Fe_2O_3, 1.41 wt.% Na_2O, and 2.49 wt.% K_2O. The results demonstrated that SiO_2 and Al_2O_3 were major components of the HF sample, in accordance with a aluminum-deficient and silicon-rich trait of black-glazed porcelain. Minor elements such as sodium, potassium and calcium existed as flux. Jian glazes were classified as high temperature calcia-iron oxide-aluminosilicate glazes, and iron oxide functioned as both flux and phase-separation accelerator during firing[27]. Previous studies indicated that[28,29], there were two kinds of microstructural forming mechanics: (1) local phase separation in glaze surface neighbouring area followed by crystallization of iron oxide, (2) crystallization of anorthite accompanied by inter-crystal phase separation and the subsequent crystallization of iron oxide.
On purpose of making further confirmation on the oxidation valence state of iron in crystalline area, the synchrotron XANES technique was employed to measure the cleaned surface. Before the experiment, spectra of iron foil (Fe), hematite (Fe_2O_3) and magnetite (Fe_3O_4) were collected as standard references, which HF sample spectra can be compared accurately. As transition metal element, iron atom has the electron configuration of $3d^6\ 4s^2$, while Fe^{3+} and Fe^{2+} correspond to $3d^5$ and $3d^6$, respectively. Fe^{3+} exhibits good stability when compared to Fe^{2+} due to electrons partially occupy the d orbit. The XANES results were illustrated in Fig. 2.

For iron foil in which the absorption K-edge was observed at 7131.2 eV, the spectrum was characterized by a small shoulder together with one inapparent crest. In post-edge region, a series of peaks turned up in succession. These characters were distinguished well between the hematite and magnetite. There was a striking pre-edge shoulder in divalent or trivalent iron, which contributed to the 1s to 3d transition. Seen from Fig. 2(b), the spectra of hematite and magnetite crystals behaved differently in the post-edge peak position. Fe_3O_4 reference showed three evident divisive crests at 7184.2, 7229.1 and 7271.8 eV, respectively. While the corresponding position in Fe_2O_3 spectrum seemed not obviously. In the HF sample result (Fig. 2a), the absorption edge peak appeared at 7133.6 eV, followed by a small shoulder at 7147.3 eV. The iron occured positive trivalent, which were consistent with the reported studies. In addition, divalent iron ions contributed to deepening the blue green of glaze surface while trivalent iron ions presented yellow. It indicated that Fe^{3+} was the color mechanism of the sample.

Table 1
Major chemical compositions of glaze and body by XRF analysis (wt.%)

	SiO_2	Al_2O_3	Fe_2O_3	Na_2O	K_2O	CaO	MgO	TiO	MnO	P_2O_5
Hare's fur glaze	62.20	16.43	8.35	N.D.	3.02	6.97	1.79	0.58	0.58	0.07
Black glaze	77.07	10.61	4.10	N.D.	2.06	3.85	1.54	0.36	0.36	0.06
Body	66.32	18.50	10.04	1.41	2.49	0.11	0.51	0.62	0.08	0.01

3.2 Microstructure analysis by OM

Figure 3 presented the surface morphology of HF sample revealed by optical microscopes. Low magnification image of the glaze surface (Fig. 3a) showed the typical characteristic of brown streak-like or silk-like hare's fur pattern. Seen from the Fig. 3b-3d, there were three types of crystal clusters in the glaze surface, one displayed a fan-shaped structure consisted of plentiful needle-like crystals; one embraced a grid structure tightly packed with plentiful spherical or irregular-shaped particles, and some white and translucent crystals were also clearly visible, which may be attributed to the residual unmelted quartz particles; the last was flower-like cluster ranging from several hundred micrometer to more than one millimeter in size. Some large-scale flower-like or fan-shaped crystals mainly aggregated at the edge of the bowl. These crystals on the surface all appeared to be brownish, which was in accordance with the appearance of hematite crystals. The cross-sectional observation showed that the glaze contained significant amounts of bubbles and crystals in the glaze-body interface and body. In addition, a brown-yellow devitrified layer appeared at the top zone of HF glaze, which may be concentrated by numerous small Fe-rich crystals.

3.3 Phase analysis by XRD and RS

With the aim of studying the crystallization behavior, the XRD pattern was performed on the glaze surface to trace the mineral composition and the relevant result was displayed in Fig. 4. Compared to the standard PDF card, the main crystalline phase was hematite (ε-Fe_2O_3) with a small amount of quartz (α-SiO_2) on the glaze. Both the thermodynamic qualification and equilibrium thermodynamic conditions for the crystallization during the firing process were conducive to the precipitation of crystals from the glaze. The porous and loose structure of porcelain body increased the concentration of dissolved oxygen and allowed the oxidation of the Fe-rich phase into hematite. The presence of unmelted quartz in the molten glaze came from the residual mineral raw materials.

To unambiguously confirm the iron oxide phases, Raman spectra carried out at different spots on the outer surface of HF glaze were shown in Fig. 5. As can be seen, the spectra taken at flower-like crystal clusters (spectrum A corresponding to Fig. 3d), fan-shaped crystal clusters (spectrum B corresponding to Fig. 3b) and honeycomb crystal clusters (spectrum C corresponding to Fig. 3c) were all identified to belong to the epsilon-hematite (ε-Fe_2O_3). ε-Fe_2O_3 phase, a rare and metastable Fe_2O_3 polymorph, has an orthorhombic crystal structure with the $Pna2_1$ space group (a=5.0810 Å, b=8.7411 Å, c=9.4083 Å)[30]. It is

defined as an intermediate between hematite (α-Fe_2O_3) and maghemite (γ-Fe_2O_3). The collected Raman peaks here shared similar peak positions at 122, 155, 234, 353, 448, 563, 689, and 1366 cm^{-1}, which were corresponding to first-order phonon vibrational modes of ε-Fe_2O_3. Majority of the detected Raman peak positions at the spectrum A, B and C matched well with each other, while few of them shifted slightly due to the faceted aspect of crystal lattice originated from the laser source (λ = 532 nm) and/or phonon confinement effect in our samples. This conclusion was consistent with the XRD observation. Beside these, we measured the phase constituent of the underlying black glaze (Fig. 5b), no other diffraction signal can be found, which implied that the black glaze was of a glassy nature.

3.4 Microstructure analysis by SEM-EDS

Figure 6 showed the morphological features of Hare's fur glaze. Based on surface observation, the boundaries between the yellow-brown Hare's fur area and black glaze area were distinct, and the chromogenic crystals on the yellow-brown Hare's fur area were uniformly distributed, as revealed in Fig. 6a. The crystals in the yellow-brown Hare's fur area can be divided into three types (hereafter, types A, B, C) on account of their sizes and microsructure, which were represented in Figure 6(b-d). With type A, the crystals inhomogenous dispersed on the streak embraced flower-shaped structure, characterized by many branches radiating from its center, petals growing along the branches and needles on both sides of the petals. This type of crystal was usually small in size. With type B, the crystals were organized orderly in dendritic-like or leaf-like manners at micrometers scales. This structure was generally accompanied by large main branches, and the secondary branches tightly arranged on the two sides of the main branch and were parallel to each other. Under the higher magnification in Fig. 6g, some large-scale dendrites were even approximately hundreds of microns and the high-order subbranches were covered by numerous intensive smaller twigs. Type C was featured as honeycomb structure closely packed with plentiful spherical or irregular-shaped crystal clusters. These crystals mainly existed in the junction zones between Hare's fur area and black glaze area.
Figure 6(e, f) presented the cross-section morphology of the HF sample. The glaze was about 1 mm thick. In comparison with the porcelain body, the glaze was rather less impure. The layer near the glaze surface contained some irregular and disordered circles or spots with higher average atomic contrast, indicated that most of the impurities was the single crystal or crystal clusters precipitated from the glaze layer, combined with a low coverage rate. Fig. 6h displayed a detailed image of the upper glaze layer. Large number of small-scale flower-shaped or feather-like crystals distributed discretely and showed a gradient variation tendency on the shape and arrangement from the glaze surface to inside.

EDS analyses performed on the glaze were shown in Fig. 7 and Fig. 8. From Fig. 7, it was manifested that the whole glaze (both the Hare's fur area and black glaze area) were mainly composed of the following elements: Al, Si, Fe, K, Ca and O. Comparatively, the element contents in the yellowish-brown Hare's fur area differed a lot from those in the black area, indicating that the phase separation have taken place in the surface glaze. Al, Fe and Ca were enriched in the yellowish-brown Hare's fur area while Si in the black glaze area. For Fe element, it had a higher concentration than that of other elements in the Hare's fur area, confirming that the chromogenic crystals in crystallization zone were ε-Fe_2O_3, which was in accordance

with previous studies. From the elemental distribution map examined on the cross sections with the depth of about 45 μm inside the glaze surface, we observed that the crystals in upper layer was much larger than that of the following part, and the content of Fe-rich crystals varied unevenly along the thickness direction. The ferric oxides gathered around the bubbles were carried to the glaze surface, causing an iron enrichment area on or beneath the surface.

Figure 9 showed the secondary electron images and corresponding magnified view of parts in the well-defined dendritic-like and leaf-like crystals. As discussed above, the dendritic crystals had a typical hierarchical structure with large main branches and parallel secondary branches on the two sides arranged symmetrically in rows. In detail, some small-scale feather-like or leafy crystal clusters aggregating at the Hare's fur streaks were mainly constitutive of acicular rods growing out the glaze surface with different lengths, as portrayed in the Figure 9(b, c). It can be observed that both ε-Fe_2O_3 crystals in the yellowish-brown Hare's fur area were all matured over the underlying black glaze layer, corroborating the previous XRD and RS results. Herein, this highly differentiated and well-bedded structure in distribution provided some useful guidance for the forming mechanism of Hare's fur pattern.

4. Discussion

In 1934, a new ferromagnetic variety of ferric oxide (ε-Fe_2O_3) was first reported by Forestier and Guillain[31]. In 1998, Tronc et al[32] gave the first detailed crystallographic structural analyses of ε-Fe_2O_3, and was later studied in 2004 by Jin et al[33]. ε-Fe_2O_3 has an orthorhombic crystal structure, is regarded as intermediate polymorph of hematite □-Fe_2O_3 and maghemite γ-Fe_2O_3[34,35]. ε-Fe_2O_3 has recently received growing attention due to its excellent magnetic properties include large coercive field, spin Seebeck effect, rapid Faraday rotation, millimeter-wave ferromagnetic resonance and coupled magnetoelectric properties[36,37]. On the side of archeological research, Dejoie et al[10] identified the presence of ε-Fe_2O_3 phase in the black-glazed Jian wares until 2014, manifested themselves in the "Hare's fur" or "oil spots" pattern. The ε-Fe_2O_3 crystals was also evidenced and documented in the ancient porcelain excavated from the Linfen kiln, Xiao kiln, Qilizhen kiln and Qingliangsi kiln.

The formation of unique HF patterns in the glaze of Jian bowls encountered as a result of the phase separation between the melted glaze and crystallized iron oxides[38]. As known, Jian wares possessed a higher iron concentration in the porcelain glaze and body. When the firing temperature in the dragon kiln reached at 1240℃, the iron minerals in the melting glaze thermally decomposed into iron oxide and released oxygen. The oxygen gathered and formed gas bubbles, which rose toward the surface with the iron-enriched melts[16,20]. When these bubbles moved out from the glaze, causing local iron enrichment. Liquid phase separation took place during the cooling procedure. As temperature continue dropped, iron oxide crystals can be precipitated due to supersaturation. Radial fur-like stripes occurred with a slower cooling rate. The HF pattern on the surface tended to be golden or yellowish-brown when fired at an oxidizing atmosphere, while silver in a reducing atmosphere. Additionally, the firing technology had a significant influence on the composition and appearance of iron-rich crystalline glaze[39]. It was generally

recognized that the firing temperature of black-glazed porcelain was between 1250℃ and 1350℃. The evolution and growth of iron crystals were affected by iron content and the dissolved oxygen content in the glaze. The higher oxygen concentration in the glaze contributed to the formation of hematite, also helped the crystals grow larger. Li et al[40,41] have pointed out that the reducing atmosphere was more conducive to the formation of ε-Fe_2O_3 phase, a mixture of stable □-Fe_2O_3 and metastable ε-Fe_2O_3 phases would come jointly in a strong oxidizing atmosphere. Moreover, Libor et al[30] found that at the SiO_2 matrix, the phase transition of γ-Fe_2O_3 to ε-Fe_2O_3 happened when the temperature rose up to 1000℃, and with an continuous improvement in temperature (~1300℃), the ε-Fe_2O_3 phase would completely transform into the □-Fe_2O_3 phase. According to the above discussion, it can be deduced that the yellowish-brown HF sample might fire between 1250℃ and 1300℃ with a weaker reducing or oxidizing atmosphere.

Based on the morphology and structure of the ε-Fe_2O_3 crystals found in the Hare's fur streaks, a possible formation mechanism of HF pattern was proposed in Fig. 10. Probably, it consisted of four steps: (1) Hematite nucleation seeds were initially formed at the gas-liquid interface of oxygen bubbles inside the glaze and gradually grew into plentiful spherical or irregular-shaped particles at the nanoscale. (2) Then these particles started to crystallize to form a two-dimensional plane structure, such as flower-shaped structure with the primary branches formed radially. (3) As the reaction time increased, more main branches such as secondary branches emerged and grew up. The longer branches quickly grew preferentially along certain directions and some began to diverge into a fan-like "petal", while the subsequent shorter branches would be blocked due to the competitive growth rates. (4) With the same growth processes, tertiary branches or other small high-order branches grew up in succession with the progressively accumulated particles attached on them, and the acicular structure tended to be thicker and thicker with the abundant raw materials and space. Eventually, the highly differentiated or well-defined hierarchical structures were formed. In general, ε-Fe_2O_3 crystals in porcelain glazes observed in previous research were mostly in three distinguishing types of appearance, one embraced dendritic or leafy structure, one had flower-shaped structure, the other was featured as honeycomb structure. Previous works have suggested that many factors like the firing temperature, cooling time, and concentration of the precursor played a crucial role in the formation of crystalline morphology. The dendritic-like and flower-like crystals usually existed in the Hare's fur area, while the crystals with honeycomb structure located at the junction zones between Hare's fur area and black glaze area.

5. Conclusion

In this work, yellowish-brown Hare's fur (HF) glazed samples were investigated by a variety of characterization methods. The morphology, chemical content and phase composition of HF glaze were presented and a possible formation mechanism of HF pattern was pointed out. The main conclusions were shown as following:

- The main constituents of the HF glaze were alumina (10.61-16.43 wt.%), silica (62.20-77.07 wt.%), calcium (3.85-6.97 wt.%) and iron oxide (4.10-8.35 wt.%). Minor elements such as sodium, potassium and calcium existed as flux. The formation of unique HF patterns in the glaze of Jian bowls encountered as a result of the phase separation between the melted glaze and crystallized iron oxides.
- There were three types of ε-Fe_2O_3 crystals in the glaze surface, one consisted of well-grown leaf-like or dendritic-like structure with highly ordered branches at micrometers scales, one was comprised of flower-like clusters accompanied by branches radiating from the center, petals growing along the branches and needles on both sides of the petals, and the last embraced a honeycomb structure tightly packed with plentiful spherical or irregular-shaped particles. In addition, ε-Fe_2O_3 crystals in the cross-section of glaze showed a gradient distribution.
- At first, the nucleation seeds were formed and gradually grew into plentiful spherical or irregular-shaped particles. Then these particles started to crystallize to form a two-dimensional plane structure, such as flower-shaped structure with the primary branches formed radially. As the reaction time increased, more main branches such as secondary branches emerged and grew up. The longer branches quickly grew preferentially along certain directions and some began to diverge. Tertiary branches grew up with the accumulated particles attached on them, following the above processes. Eventually, a highly differentiated or well-defined hierarchical structures were formed.

Declarations

Conflicts of Interest:

The authors declare that they have no known competing financial interests or personal relationships that could have appeared to influence the work reported in this paper.

Acknowledgments:

This research was supported by the National Key R&D Program of China (grant number: 2019YFC1520203).

References

1. X. Chen, S. Chen, R. Huang, et al. A study on Song dynasty Jian bowl [J]. China Ceramics, 1983, 2: 61-69 (in Chinese).
2. R. Huang, X. Chen, S. Chen, et al. A high resolution electron microscopic investigation on the imitative glaze of Yaobian Tenmoku in Southern Song Dynasty (in Chinese), China Ceramics, 1988, 1: 17-21.
3. X. Li, J Lu, X. Yu, et al. Imitation of ancient black-glazed Jian bowls (Yohen Tenmoku): Fabrication and characterization [J]. Ceramics International, 2016, 42: 15269-15273.

4. C. Xu, W. Li, X. Lu, et al. Unveiling the science behind the tea bowls from the Jizhou kiln. Part I. Chemical compositions and the two-layer glazing technique [J]. Ceramics International, 2018, 44(7): 8540-8549.
5. W. Li, W. Zhang, X. Lu, et al. Chemical compositions and microstructures of hare's fur black-glazed porcelains from Jian kiln, Jizhou kiln and Yaozhou kiln sites [J]. Journal of Building Materials, 2011, 14: 329-334 (In Chinese).
6. Z. Liu, Z. Zhang, H. Li, et al. Microstructure characteristics of the black-glazed shreds excavated from the Qingliangsi Kiln [J]. Key Engineering Materials, 2012, 492: 112-117.
7. A. Zhang. Scientific research on Jianzhan in Song Dynasty [J]. Ceramics, 2021, (05), 157-158.
8. N. Chen. Taking the Hare's fur glazed bowls as an example, discussing the firing process of Jian wares (In Chinese). Oriental Collection, 2020, 06: 48-50.
9. X. Chen, J. Sun, Discussion on the peculiarity of oil spot national treasure Tenmoku Wares Jian of spot through the research results of the rare sherds, J.Ceram. (1995) 26.
10. C. Dejoie, P. Sciau, W. Li, et al. Learning from the past: Rare ε-Fe_2O_3 in the ancient black-glazed Jian (Tenmoku) wares [J]. Scientific Reports, 2014(4): 1-9.
11. M. Gich, C. Frontera, A. Roig, et al. Magnetoelectric coupling in ε-Fe_2O_3 nanoparticles [J]. Nanotechnology, 2006, 17: 687-691.
12. K. Knížek, M. Pashchenko, P. Levinský, et al. Spin seebeck effect in ε-Fe_2O_3 thin films with high coercive field [J]. Journal of Applied Physics, 2018, 124.
13. Y. Ding, J.R. Morber, R.L. Snyder, et al. Nanowire structural evolution from Fe_3O_4 to ε-Fe_2O_3 [J]. Advanced Functional Materials, 2007, 17: 1172-1178.
14. J. Tuček, R. Zbořil, A. Namai, et al. ε-Fe_2O_3: an advanced nanomaterial exhibiting giant coercive field, millimeter-wave ferromagnetic resonance, and magnetoelectric coupling [J]. Chemistry of Materials, 2010, 22(24): 6483-6505.
15. Y. Kusano, T. Fujii, J. Takada, et al. Epitaxial growth of ε-Fe_2O_3 on mullite found through studies on a traditional Japanese stoneware [J]. Chemistry of Materials, 2008, 20: 151-156.
16. Q. Hoo, Y. Liang, X. Yan, et al. Millimeter-sized flower-like clusters composed of mullite and ε-Fe_2O_3 on the Hare's Fur Jian Ware [J]. Journal of the European Ceramic Society, 2020, 40: 4340-4347.
17. G. Franci, T. Akkas, S. Yildirim. Characterization of a Jian-like sherd with the optical microscope, confocal Raman, wavelength-dispersive X-ray fluorescence, and portable XRF spectrometers [J]. Journal of Raman Spectroscopy, 2020(51): 1-10.
18. L.Wang, Y Wang, M. Zhang, et al. Three-dimensional microstructure of ε-Fe_2O_3 crystals in ancient Chinese sauce glaze porcelain revealed by focused ion beam scanning electron microscopy [J]. Analytical chemistry, 2019, 91: 13054-13061.
19. M. Wang, T. Wang, F. Wang, et al. Raman study of rusty oil spotted glaze produced in Linfen kilns (Shanxi province, AD 1115-1368) [J]. Journal of Raman Spectroscopy, 2021, 1-11.

20. Y. Xu, Y Qin, F. Ding. Characterization of the rare oil spot glazed bowl excavated from the Xiao kiln site of north China [J]. Ceramics International, 2017, 43: 8636-8642.
21. C. Xu, W. Li, X. Lu, et al. Unveiling the science behind the tea bowls from the Jizhou kiln. Part II. microstructures and the coloring mechanism [J]. Ceramics International, 2018, 44(16): 19461-19473.
22. R. Wen, D. Wang, L. Wang, Y. Dang, The colouring mechanism of the brown glaze porcelain of the Yaozhou Kiln in the Northern Song Dynasty [J]. Ceramics International, 2019, 45: 10589-10595.
23. D. Zhong, M. Guo, Y. Liu, et al. Nondestructive analysis of iron rich porcelains excavated from Qingliangsi Site in Baofeng Country, Henan Province [J]. Spectroscopy and Spectral Analysis, 2019, 1: 172-179 (in Chinese).
24. Z. Liu, C. Jia, L. Li, et al.The morphology and structure of crystals in Qing Dynasty purple-gold glaze excavated from the Forbidden City [J]. Journal of the American Ceramic Society. 2018, 101(11): 5229-5240.
25. S. Liu, Q. Li, F. Gan, et al. Characterization of some ancient glass vessels fragments found in Xinjiang, China, using a portable energy dispersive XRF spectrometer [J]. X-Ray Spectrometry, 2011, 40(5), 364-375.
26. S. Liu, Q. Li, F. Gan, et al. Silk Road glass in Xinjiang, China: chemical compositional analysis and interpretation using a high-resolution portable XRF spectrometer [J]. Journal of Archaeological Science, 2012, 39(7), 2128-2142.
27. Y. Min. The development of ancient iron-based glaze and its Impact, Jingdezhen Ceramic Institute, 2009 (in Chinese).
28. W. Li, H. Luo, J. Li, et al. Studies on the microstructure of the black-glazed bowl sherds excavated from the Jian kiln site of ancient China [J]. Ceramics International, 2008, 34: 1473-1480.
29. Z. Liu, Z. Zhang, H. Li, et al. Microstructure characteristics of the black-glazed shreds excavated from the Qingliangsi Kiln [J]. Key Engineering Materials, 2012, 492: 112-117.
30. M. Libor, T. Jiri, Z Radek. Polymorphous Transformations of Nanometric Iron (III) Oxide: A Review [J]. Chemistry of materials, 2011, 23: 3255-3272.
31. Forestier, H.& Guiot-Guillain, G. New ferromagnetic variety of ferric oxide [J]. C. R. Acad. Sci. (Paris), 199, 720 (1934).
32. E. Tronc, C. Chaneác, J.P. Jolivet. Structural and magnetic characterization of ε-Fe_2O_3, (1998).
33. J. Jin, S.Ohkoshi, K. Hashimoto. Giant coercive field of nanometer-sized iron oxide [J]. Advanced Materials, 2004, 16(1): 48-51.
34. D. L. A. de Faria, Venaü ncio Silva, de Oliveira. Raman microspectroscopy of some iron oxides and oxyhydroxides [J]. Journal of Raman Spectroscopy, 1997, 28: 873-878.
35. J. López-Sánchez, A. Serrano, A. Del Campo, et al. Sol-Gel synthesis and Micro-Raman characterization of ε-Fe_2O_3 micro- and nanoparticles [J]. Chemistry of Materials, 2016, 28: 511-518.
36. GA. Bukhtiyarova, MA. Shuvaeva, OA. Bayukov, et al. Facile synthesis of nanosized ε-Fe_2O_3 particles on the silica support [J]. Journal of Nanoparticle Research, 2011, 13(10): 5527-5534.

37. E. Taboada, M. Gich, A. Roig. Nanospheres of silica with an epsilon-Fe_2O_3 single crystal nucleus [J]. Acs Nano, 2009, 3(11): 3377.
38. P. Shi, F. Wang, J. Zhu, et al. Effect of phase separation on the Jian ware blue colored glaze with iron oxide [J]. Ceramic International, 2018, 44(14): 16407-16413.
39. W. Zhang, N. Zheng, W. Li. Scientific study of high-iron crystallization glaze (in Chinese)., China Ceramics, 2010, 46(8): 20-25.
40. S. Lahlil, J. Xu , W. Li. Influence of manufacturing parameters on the crackling process of ancient Chinese glazed ceramics [J]. Journal of Cultural Heritage, 2015, 16: 401-412.
41. M. Li, W. Li, X. Lu, et al. Controllable preparation and decorative effect of iron-based crystalline glazes [J]. Journal of the Chinese Ceramic Society, 2020, 48(7): 1134-1144.

Figures

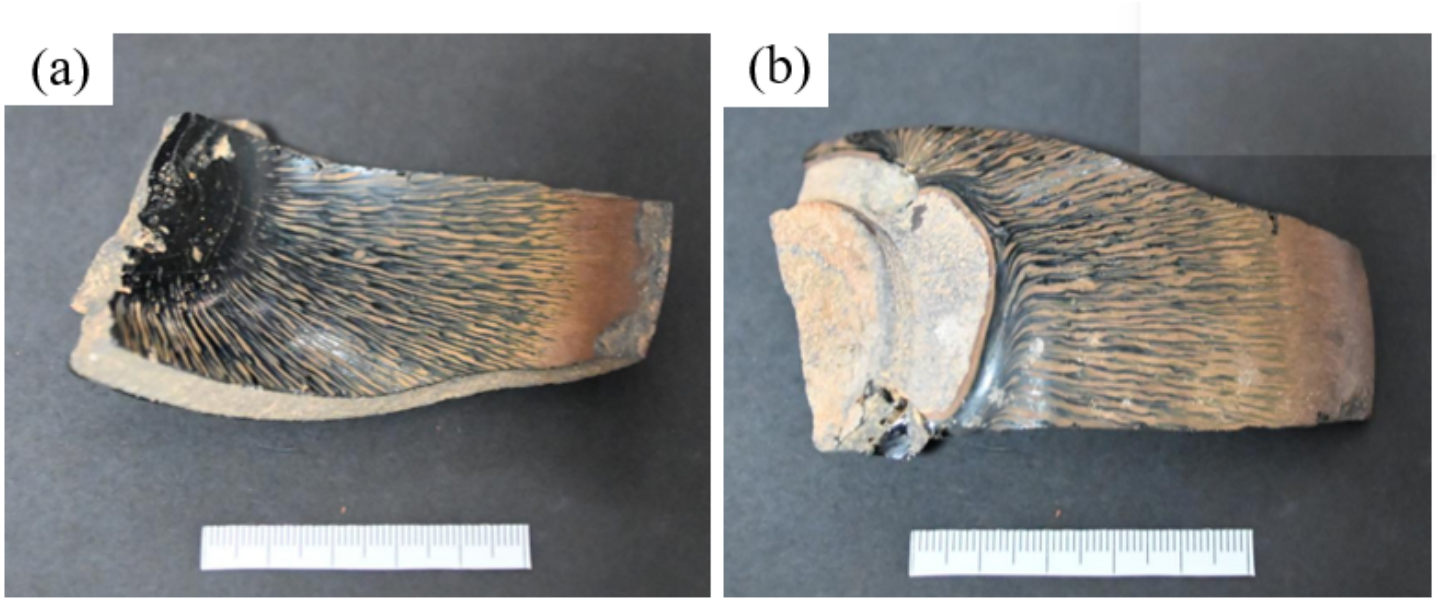

Figure 1

The Hare's fur Jian ware in Fujian Province, China

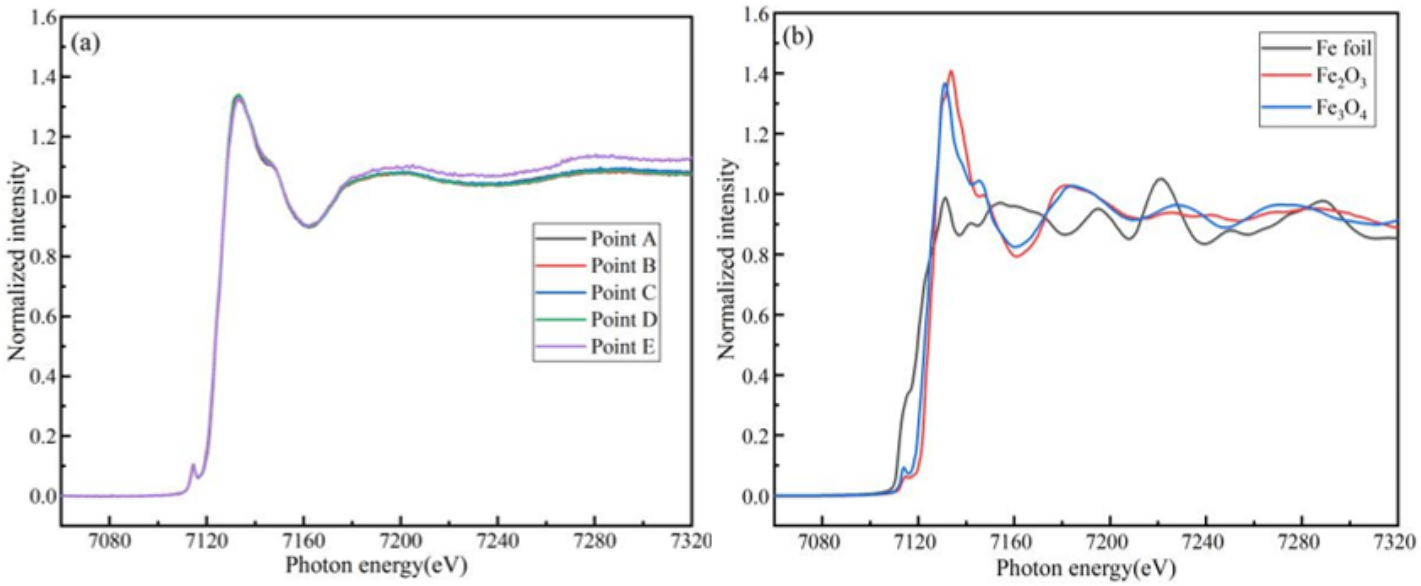

Figure 2

Fe K-edge XANES spectra: (a) the HF sample (Points A, B, C, D, E are corresponding to the crystallization zone); (b) standard spectra of iron foil (Fe), hematite (Fe2O3) and magnetite (Fe3O4).

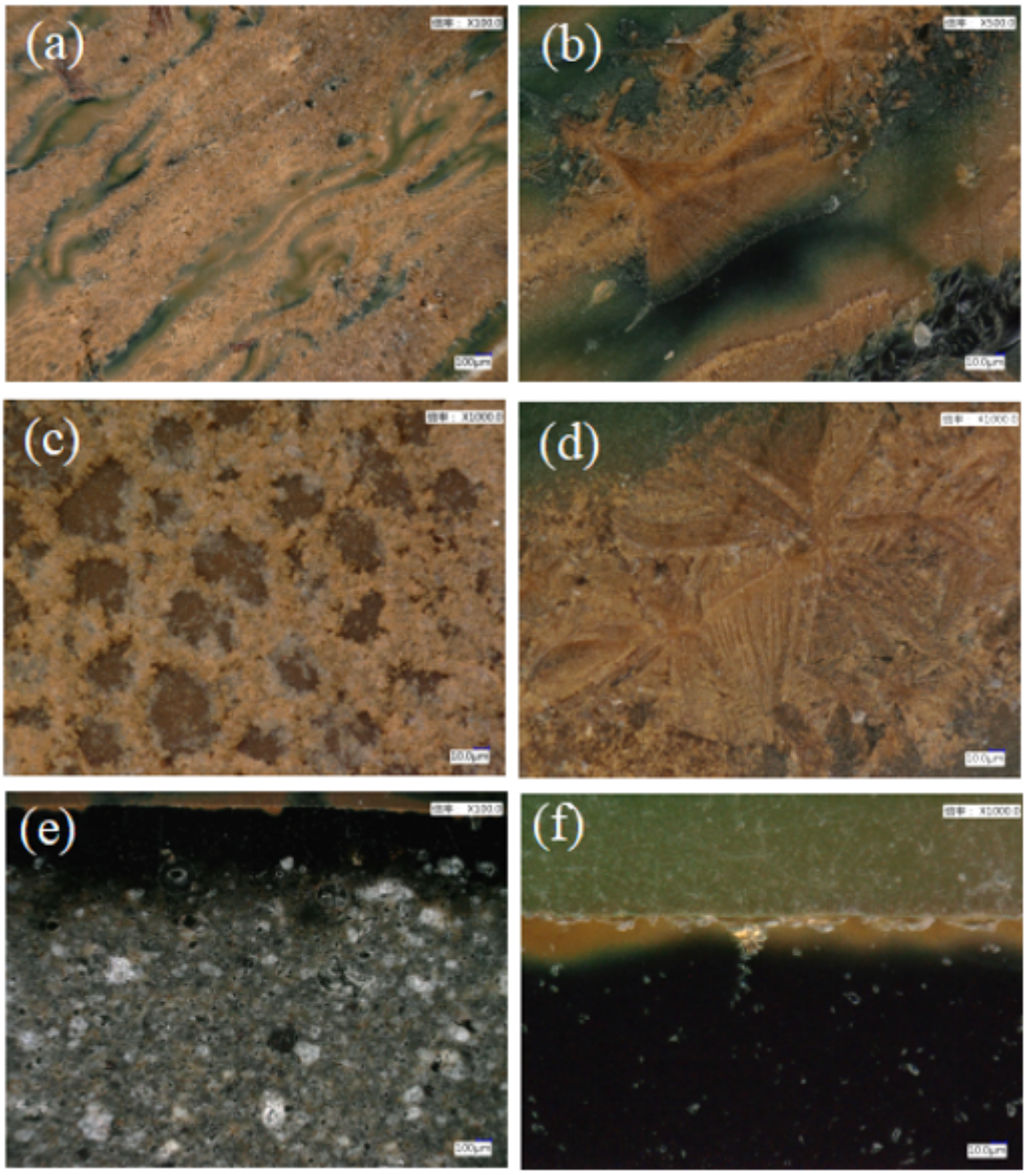

Figure 3

Optical observation of the HF sample with different magnification: (a-d) the glaze surface, (e, f) the polished cross-section.

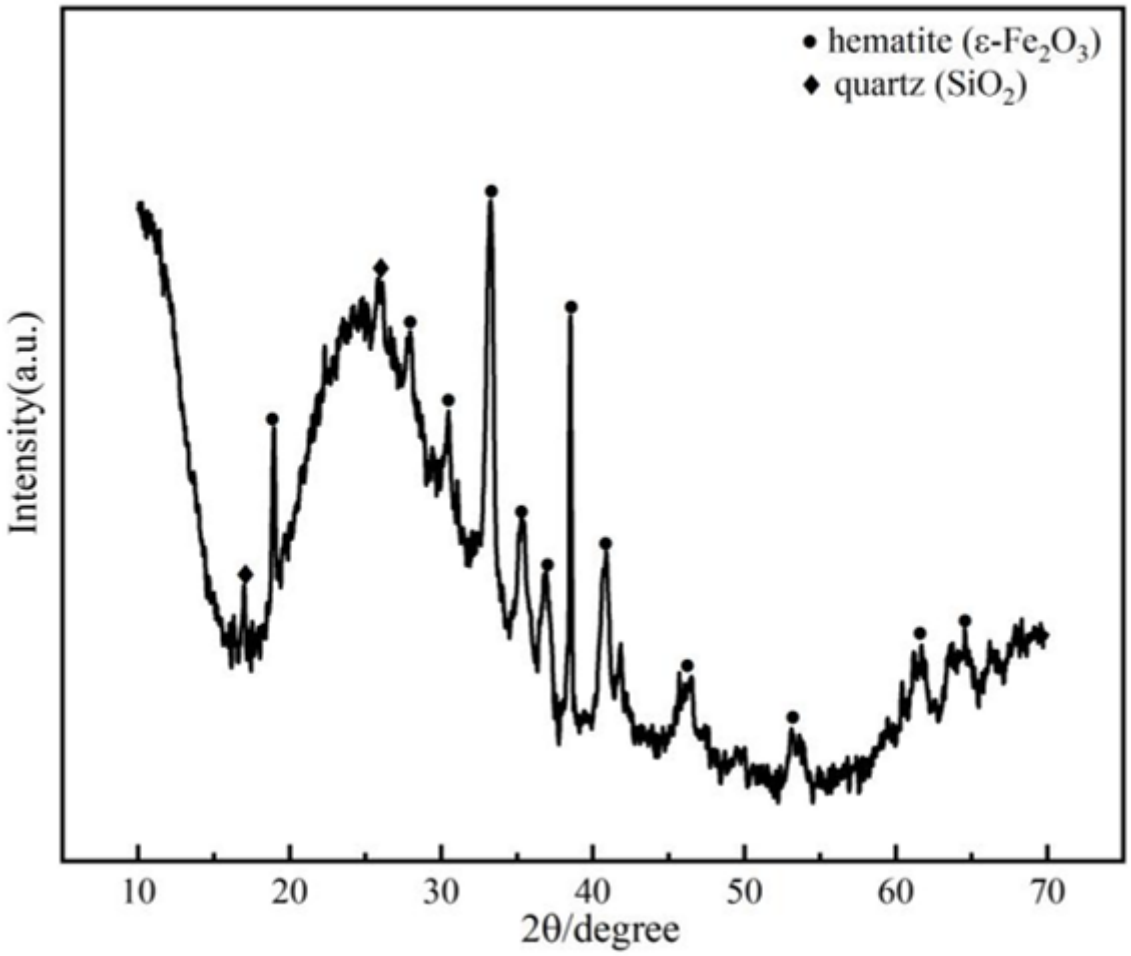

Figure 4

XRD pattern of the glaze surface.

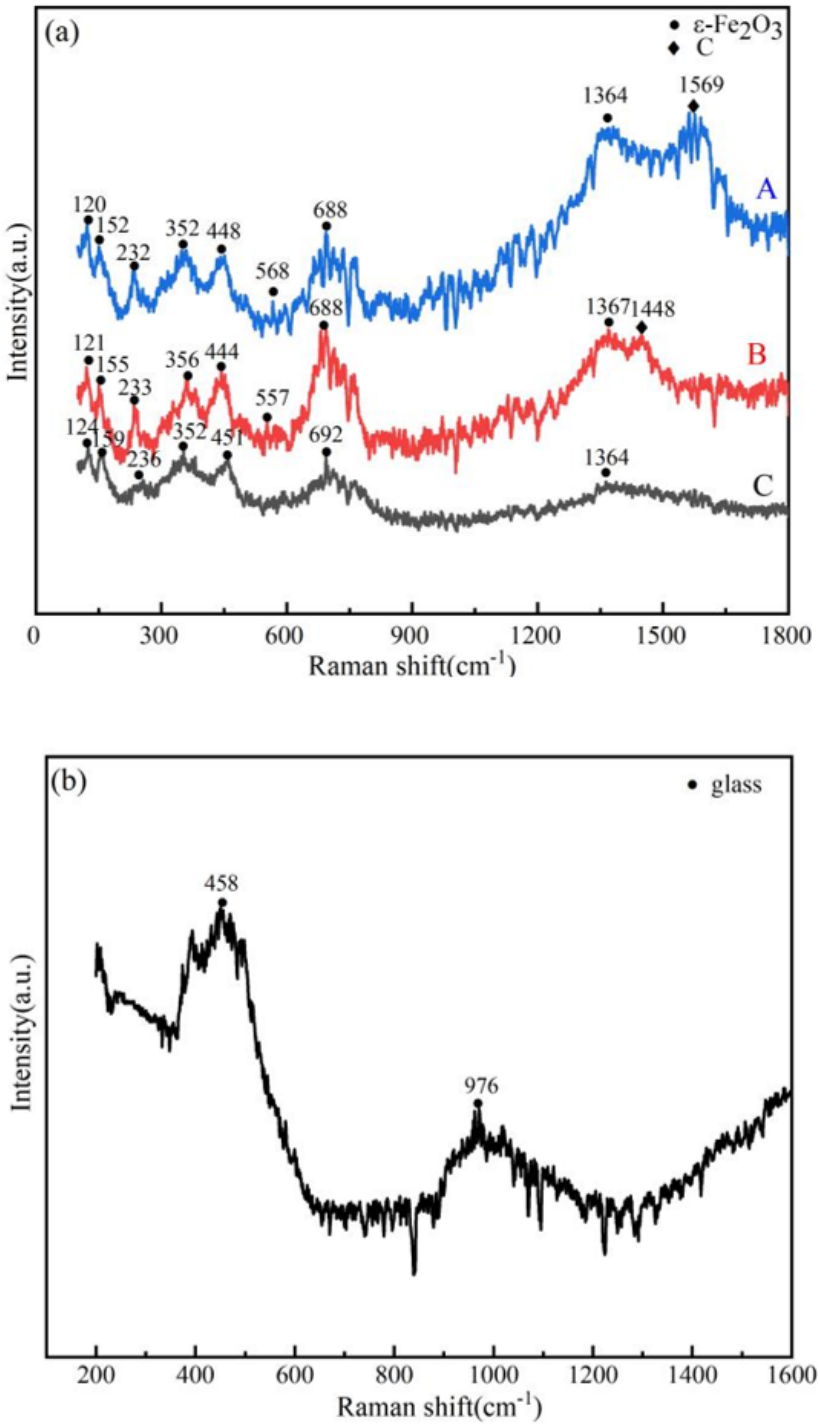

Figure 5

Raman spectra of the sample: (a) different spots at the yellowish-brown hare's fur area, (b) black glaze area.

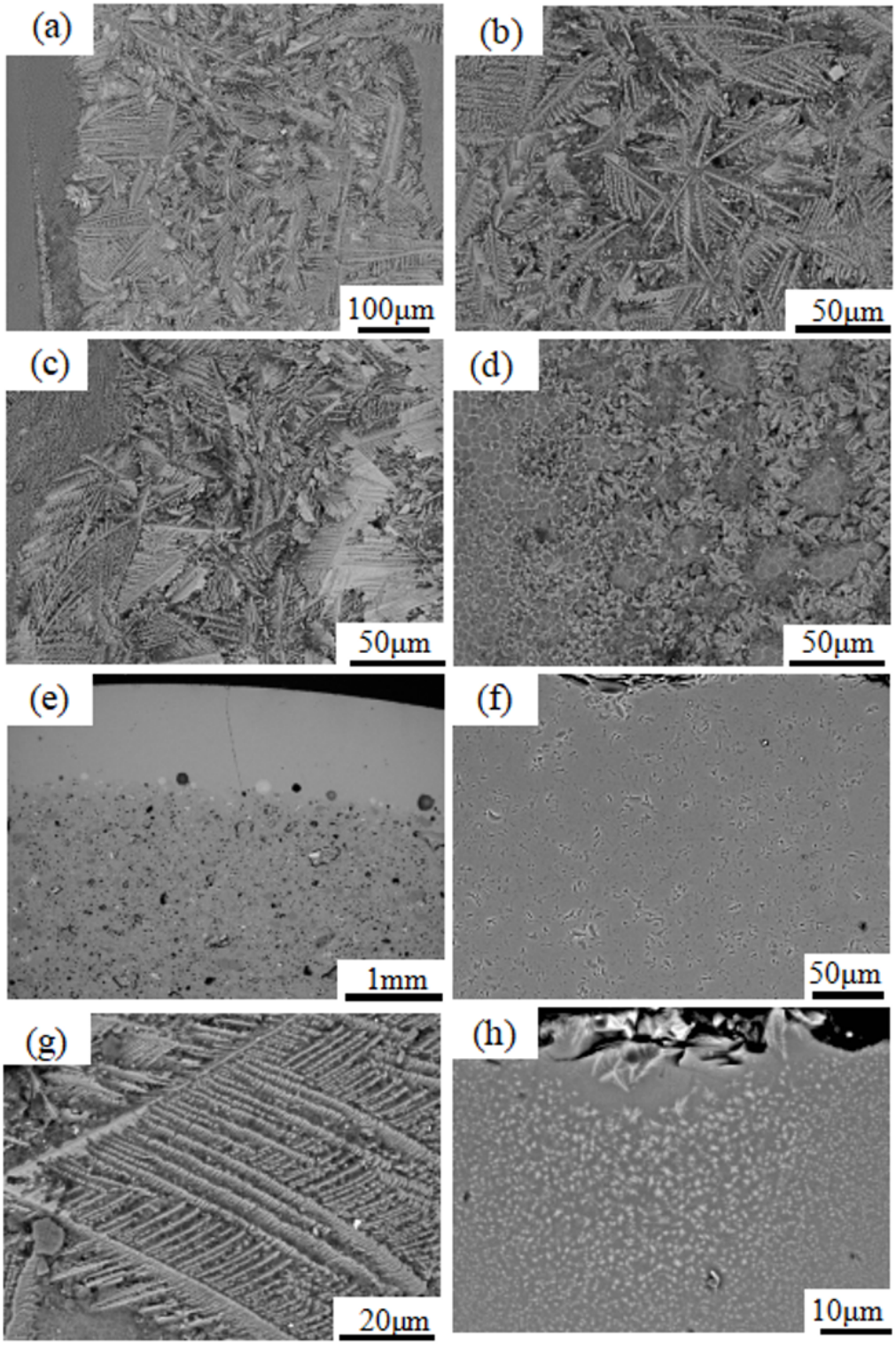

Figure 6

SEM images of the HF glaze with different magnification: (a, b, c, d, g) surface morphology, (e, f, h) the polished cross-section morphology.

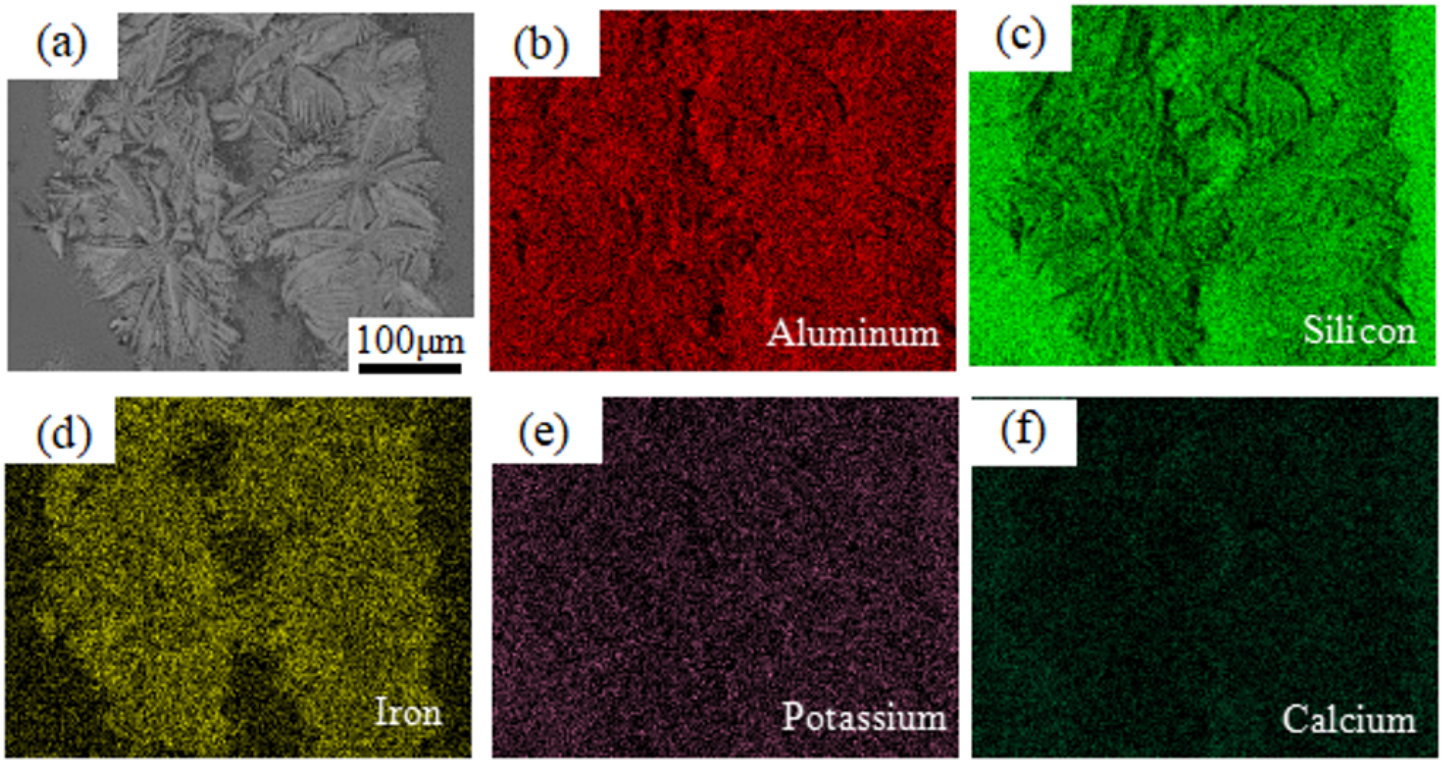

Figure 7

The element map distribution results of the surface glaze.

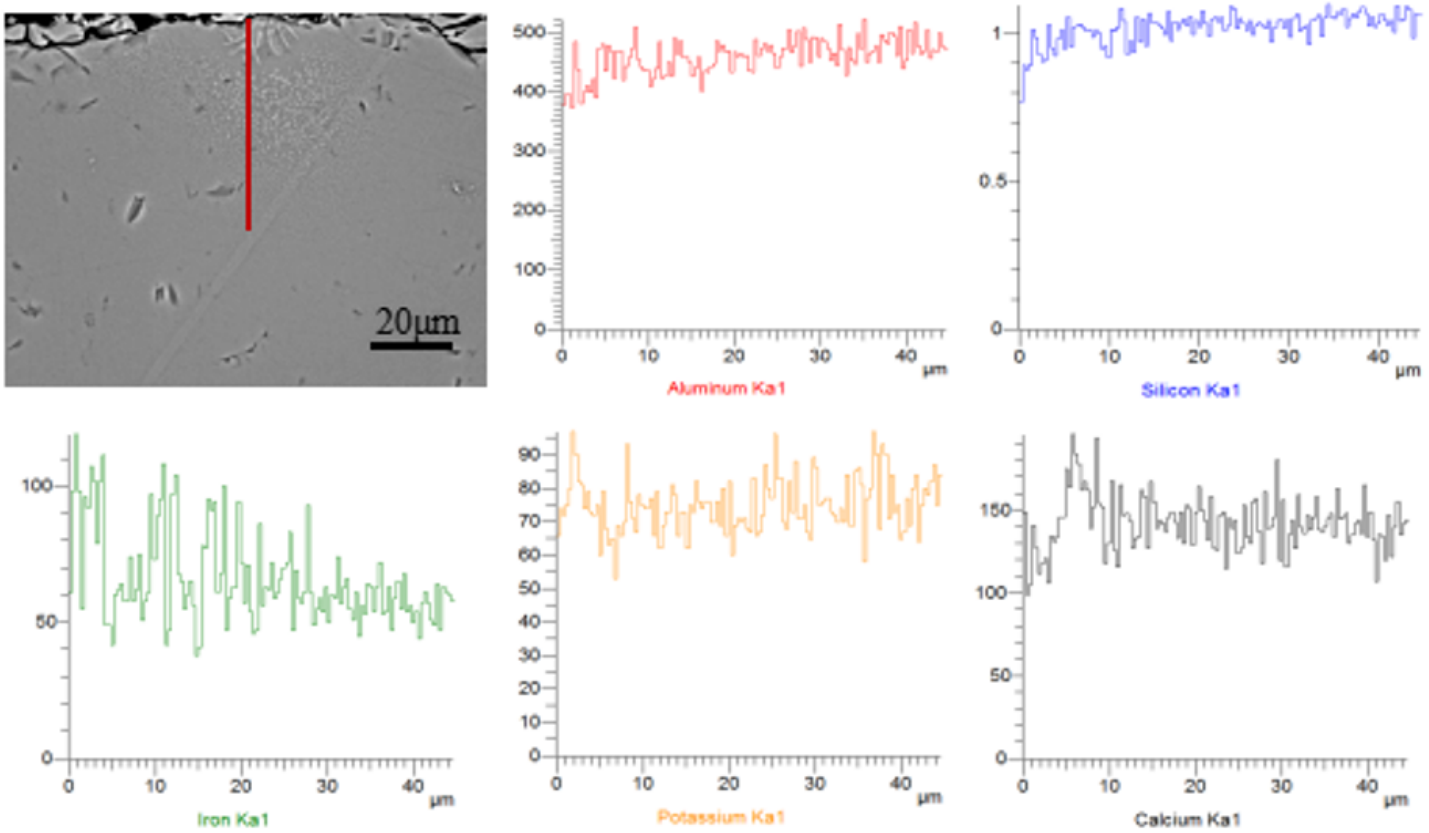

Figure 8

The element map distribution results of the polished cross-section.

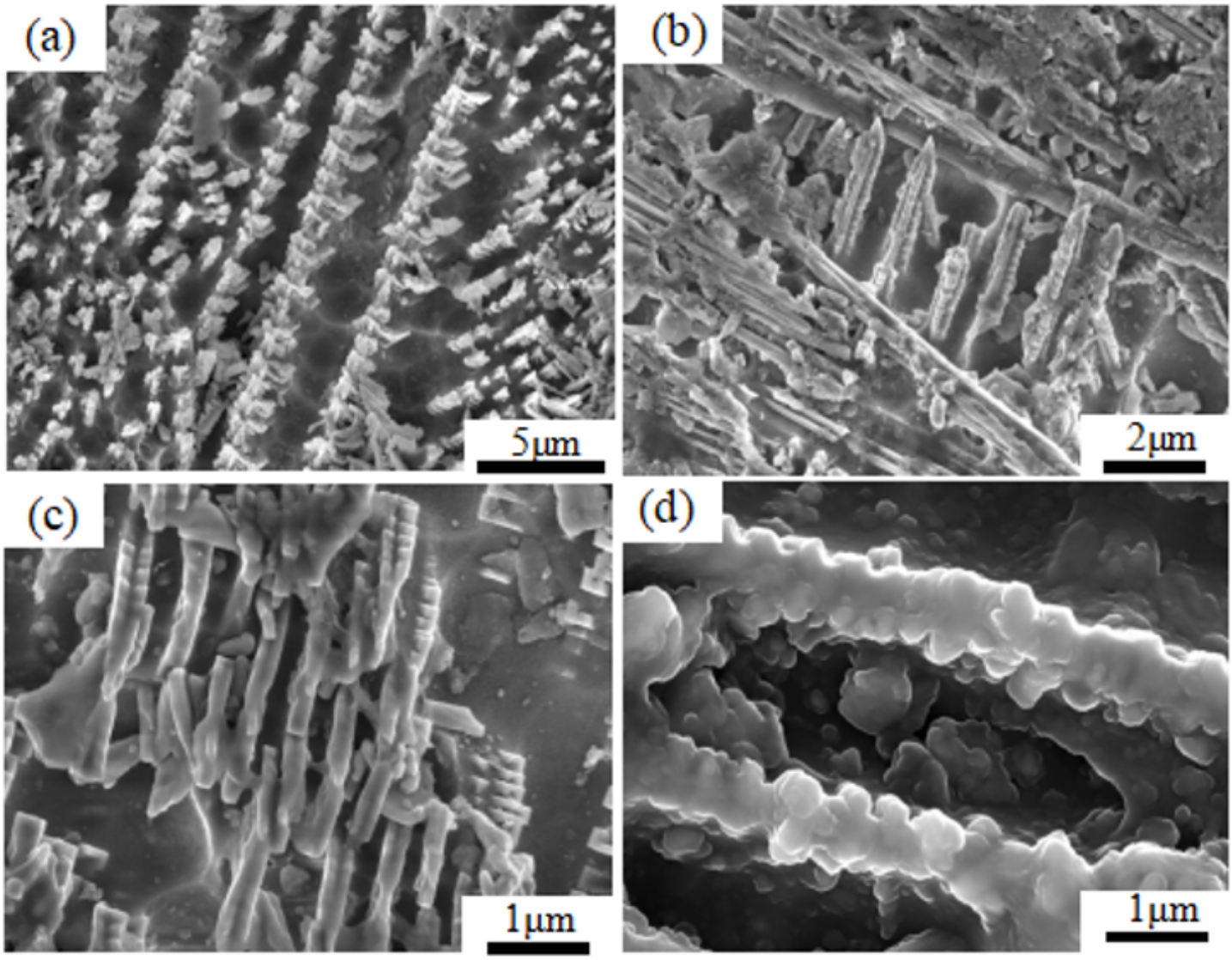

Figure 9

Secondary electron image of crystals on the glaze surface.

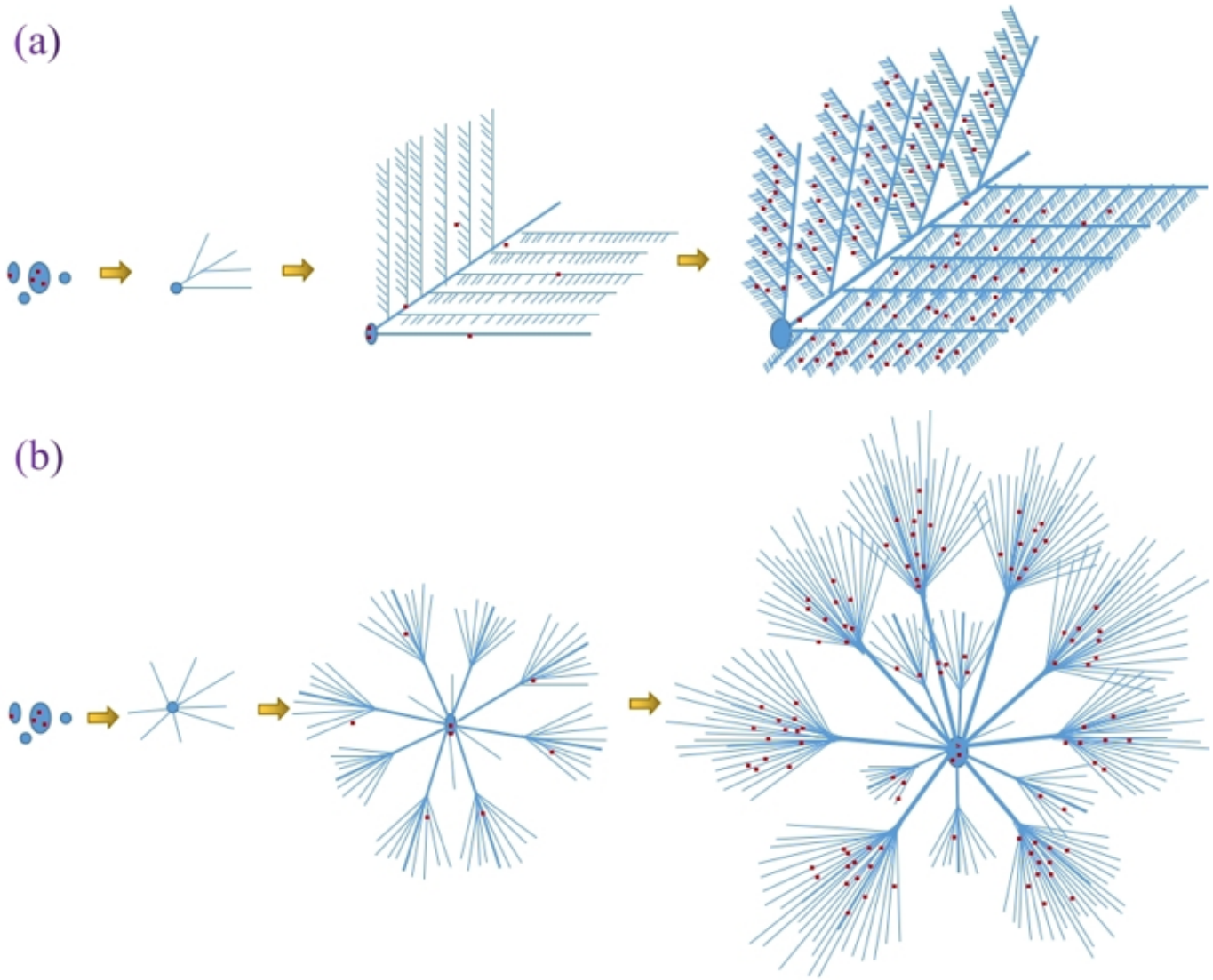

Figure 10

A possible formation mechanism of HF pattern. (a) dendritic-like crystals, (b) flower-like crystals.